Hollow Nanoneedle Array and Its Utilization for Repeated Administration of Biomolecules to the Same Cells

Elad Peer,[†] Arbel Artzy-Schnirman,[†] Lior Gepstein,[†,‡] and Uri Sivan[†,§,*]

[†]Russel Berrie Nanotechnology Institute, [‡]Rappaport Faculty of Medicine and Research Institute, and [§]Department of Physics, Technion-Israel Institute of Technology, Haifa 32000, Israel

ABSTRACT

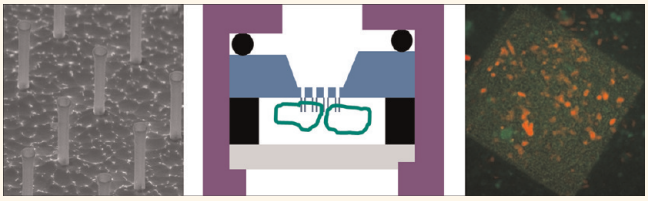

We present a novel hollow nanoneedle array (NNA) device capable of simultaneously delivering diverse cargo into a group of cells in a culture over prolonged periods. The silica needles are fed by a common reservoir whose content can be replenished and modified in real time while maintaining contact with the same cells. The NNA, albeit its submicrometer features, is fabricated in a silicon-on-insulator wafer using conventional, large scale, silicon technology. 3T3-NIH fibroblast cells and HEK293 human embryonic kidney cells are shown to grow and proliferate successfully on the NNAs. Cargo delivery from the reservoir through the needles to a group of HEK293 cells in the culture is demonstrated by repeated administration of fluorescently labeled dextran to the same cells and transfection with DNA coding for red fluorescent protein. The capabilities demonstrated by the NNA device open the door to large scale studies of the effect of selected cells on their environment as encountered, for instance, in the study of cell-fate decisions, the role of cell-autonomous *versus* nonautonomous mechanisms in developmental biology, and in the study of excitable cell-networks.

KEYWORDS: nanoneedles · plasma etching · fabrication · self aligned · hollow · saponin · NIH3T3 · HEK293 · transfection · administration

Cargo delivery into living cells presents considerable challenge in biological and medical research. Traditional delivery strategies[1] such as viral vectors and electroporation are random in nature, potentially toxic or traumatic to cells, and do not allow continuous or repeated delivery of molecules to the same cells in a culture. Microinjection, albeit being specific, suffers from low throughput[2,3] due to its serial nature, requires skilled personnel, and is often traumatic to cells. None of these methods hence facilitates safe, repeated administration of molecules to the same cells in a culture.

Recent advances in nanotechnology enable new strategies that meet this goal. They facilitate cargo delivery into living cells[4−12] as well as probing of the cell response to these cargoes.[13−17] Some promising techniques use either hollow[9,18−21] or solid[5−7,10,12,13,16,17,22−24] pillar geometries. Atomic force microscope (AFM) equipped with a sharp tip has been used by several groups to puncture single cells and insert substances directly into the cytoplasm.[19,22,25−30] Others have attempted to integrate standard microinjection tools with microfluidic systems,[31] or to load cargo into hollow nanostructures,[9] and use these structures to later penetrate cells and release the cargo in the cytoplasm. Simultaneous administration of substances to multiple cells in a culture has been addressed by nanopillar arrays[5,6,9,10,12] on which cells were grown. Solid and hollow carbon nanofibers have been shown to penetrate cells,[4,8,9,11,25] and silicon nanowires have been used by several groups[5,12] to penetrate cells and deliver cargo.

The techniques listed above were all "single-shot", namely, facilitated one-time administration of preloaded molecules to cells in a culture. Consecutive administration of different molecules to the same group of cells, or even repeated administration of the same molecules, is cumbersome with the AFM and microinjection techniques and becomes practically impossible with the various hollow or solid pillar array configurations. Two barriers impede the development of such a capability along the lines taken in the above studies: Injector reloading and a method for repeated injection to the same cells while maintaining

* Address correspondence to phsivan@tx.technion.ac.il.

Received for review January 30, 2012 and accepted May 26, 2012.

Published online May 26, 2012
10.1021/nn300443h

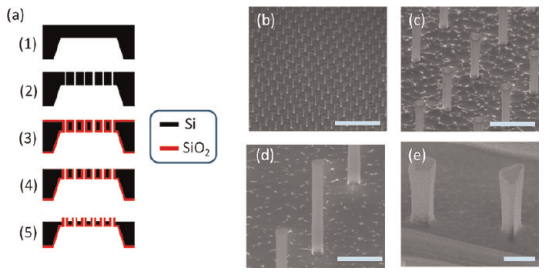

Figure 1. Nanoneedle array. (a) Schematics of the fabrication process. (1) Thin silicon membranes were realized in an SOI wafer using optical lithography and selective etching. (2) The membranes were perforated where needles were desired. (3) The perforated membranes were oxidized. (4) The front oxide layer was removed, exposing the underlying silicon. (5) The exposed silicon membrane was partially etched, leaving hollow oxide needles connected to the back reservoir. (b) Overview of a *ca.* 100 μm $\times$ 100 μm field of nanoneedles defined on the silicon membrane. (c) Magnified view of the array presented in panel a reveals the 5 μm spacing between needles and their height (5 μm). (d) Details of a single silica nanoneedle. (e) Square and triangular nanoneedles fabricated by a corresponding e-beam patterning and the same fabrication process. Needles of various cross sections can be mixed on the same die. Scale bars: (b) 20 μm, (c) 3 μm, (d) 2 μm, (e) 2 μm.

their integrity and vitality. The first gap can be mitigated by utilizing nanoneedles fed by a reservoir,[32,33] but the second challenge requires either repeated puncturing of multiple cells or fusion of the nanoneedles with the cell's membrane for prolonged times. Repeated puncturing is technically complex in the case of multiple cells treated by an extensive nanoneedle array while fusion of nanoneedles with the cells might affect the cells wellbeing over extended periods, not to mention difficulties in keeping the needles' lumen clear of clogging by actin and other macromolecules.

In the present manuscript, we offer solution to these challenges. In the first part, we present a novel fabrication technique that yields hollow nanoneedle arrays (NNA) of desired shape, size, and position, all fed by a common reservoir. The NNA are fabricated by conventional silicon technology, rendering them amenable to volume production. In the second part, we employ these arrays to demonstrate repeated administration of DNA and other biomolecules to the same group of HEK293 cells in a culture, while maintaining the cells integrity and viability over prolonged periods. Biomolecules are administered to cells growing on the NNA by mixing them with the membrane permeation promoter saponin and applying the solution to the common reservoir, from which the molecules diffuse through the needles and reach the cells' cytoplasm. The needles in our system play several roles: they serve to improve the membrane permeability in the presence of saponin, to maintain a concentration gradient of saponin and target molecules between the needle's lumen and the bulk solution, and to direct the target molecules to specific locations in the culture.

RESULTS

Nanoneedles Fabrication. The five-step fabrication process is outlined in Figure 1a. Details can be found in the Supporting Information, section S1. First, 10 μm thick silicon membranes are realized in a silicon-on-insulator (SOI) substrate using optical lithography and wet etching of the back side of the substrate (Figure 1a-1). The membranes are then perforated at desired places (Figure 1a-2) using e-beam lithography and deep reactive ion etching (DRIE). The perforated membranes are thermally oxidized (Figure 1a-3) to coat the pores created in the previous stage with silicon dioxide. Subsequently, the top oxide layer is removed by directional plasma etching, exposing the top surface of the silicon membrane (Figure 1a-4). Finally, the exposed silicon membrane is thinned down from 10 μm to *ca.* 5 μm using selective ion etching tuned to remove silicon considerably faster than silica (Figure 1a-5). As the top surface of the silicon membrane etches away, the once buried silica coating of the pores turns into hollow needles extending from the front surface of the thinned silicon membrane. By construction, the nanoneedles are connected to a common reservoir at the back. The process is self-aligned, depending solely on selective etching of silicon relative to silica. In terms of robustness, versatility, and control over the nanoneedles geometry and distribution, it offers some advantages over the GaAs-based technique reported in ref 32.

The resulting nanoneedle arrays, fabricated by the aforementioned process on a 13 mm $\times$ 13 mm SOI die, are depicted in Figure 1b–e. The nanoneedles, spaced by 5 μm, form a 300 μm $\times$ 300 μm array (Figure 1b,c). Each needle is 5 μm tall and 0.5 μm wide (Figure 1d). Its 250 nm diameter lumen traverses the 5 μm thick supporting silicon membrane. Additionally to the hollow nanoneedle array defined on top of the 300 μm $\times$ 300 μm membrane, the die (device) contains, for testing purposes, a domain of needles fabricated using the same process on top of the solid wafer. These needles are therefore disconnected from the common reservoir. Each NNA die hence displays to the cells three domains: hollow needles array, blocked needles array presenting the same topography as the hollow needles, and flat, natively oxidized silicon.

Passing Molecules through the Needles. Molecule transfer through the nanoneedles was evaluated using fluorescin (Sigma-Aldrich), 3kD Texas-Red labeled dextran (Sigma-Aldrich), and double-stranded DNA plasmid (5.2 kbp plsRes2-DsRed-Express plasmid, Clontech). A NNA die was placed in a sample holder built in-house (see Figure 2a and Supporting Information S2 for detailed description) with its front side immersed in 50 μL phosphate buffer saline (PBS). The sample holder was placed on an inverted microscope (Zeiss Axiovert200) with the needles facing down, and 200 μL solution containing target molecules in PBS was added to the

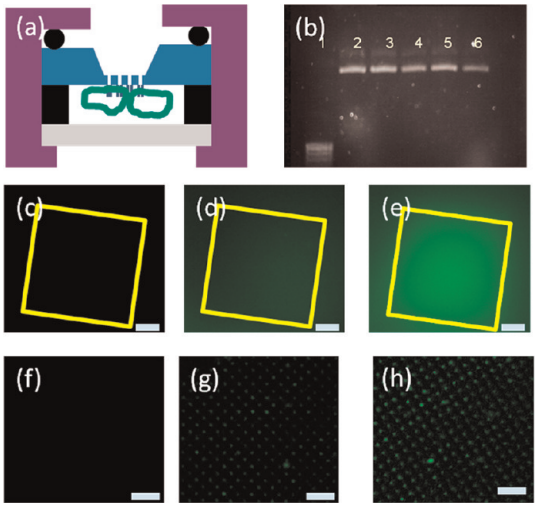

Figure 2. Molecule passage through nanoneedles. (a) Schematic cross-section of a NNA device assembled in the home-designed sample holder. The NNA chip (blue) is placed with the needles and preincubated cells (green) facing down to the observation window (gray). The device is sealed by "O"-rings (black) which are pressed against a mechanical support (purple). The reservoir is accessible through a hole in the mechanical support (visible on the top of the panel). (b) Gel electrophoresis confirming passage of the 5.2 kbp plasmid plsMSCVPuro through the NNA. Lane 1: ssDNA probe molecules. Lane 2: source solution containing the plasmid. Lanes 3, 5: solution collected from the reservoirs of two duplicates after 2 h incubation. Lanes 4, 6: solution collected from the front side of two duplicate NNA dies after 2 h incubation. (c–h) Fluorescin passage through the NNA as imaged by fluorescence microscopy. (c–e) Image of the bulk solution above the needles, before fluorescin addition to the reservoir (c), immediately after fluorescin addition to the reservoir (d), and 15 min after fluorescin addition to the reservoir (e). (f–h) Confocal microscope image of a plane (*z*-section) along the needles' body, before addition of fluorescin to the reservoir (f), immediately after addition of fluorescin to the reservoir (g), and 30 s after addition of fluorescin to the reservoir (h). Scale bars: (c) 50, (d) 50, (e) 50, (f) 15, (g) 15, (h) 15 μm.

back reservoir. The sample holder allowed an easy access to the reservoir while the device was mounted on the inverted microscope stage. The transfer of molecules through the needles was driven by diffusion alone, with no external pressure (see Supporting Information-section S3). When passing DNA plasmid, the solution at the front side of the die was collected after 120 min and run in 1% agarose gel. As depicted in Figure 2b, a clear band corresponding to the injected DNA appeared, proving DNA transport from the reservoir through the needles to the solution at the front side of the die.

When passing fluorophores, an easily detectable fluorescence signal appeared within minutes in the needles' openings, spreading into the solution at the front side of the NNA (Figure2c–h and Supporting Information, movie S4).

Cell Culturing on NNA Dies. HEK293 human embryonic kidney cells and NIH3T3 mouse fibroblast cells expressing eGFP were cultured on the NNA dies. Twenty-four hours after seeding, both cell types spread and formed a viable culture. Cell growth, 24 to 48 h after seeding, was evaluated by time-lapse microscopy (Supporting Information, movie S4). As seen in S4, the cells were able to move and proliferate on the NNA dies, with no apparent preference to a specific domain on the die. We next performed quantitative analysis of the ability of cells to grow and proliferate when cultured on NNA dies containing either open or closed nanoneedles, flat silicon domains, and control tissue-culture plates. The resulting cell growth curves (Figure 3a) revealed comparable increase in the number of cells over time in all cases.

As seen in Figure 3b–d and in Supporting Information, Figure S5, the cells grew around the needles and not merely above them. This fact was verified using both confocal microscopy (Zeiss LSM510) and SEM imaging of cells fixated on the NNA dies (using the electron beam of a dual beam Strata400S FIB). The confocal image presented in Figure 3b clearly shows that the nuclei of HEK293 cells were localized within the volume between and around the nanoneedles. Moreover, the nanoneedles did not seem to interfere with the cells' well-being and division (circled cell in Figure 3b, and Supporting Information, movie S6).

SEM images of NIH3T3 cells fixated on the NNA die (Figure 3c,d) indicated that cells tend to spread on the upper section of the NNA without reaching down to the substrate. This result is evident in Figure 3c, where cells at the border of the NNA seem to "climb" the needles, and in Figure 3d showing a hovering cell body wrapped around the top of a nanoneedle. The needles were thus found to form close contact with the cell membrane but we were unable to judge whether they physically punctured the membrane and penetrated into the cell cytoplasm.

Administration of Fluorescently Tagged Dextran to Cells. HEK293 cells were grown on the NNA dies for 48 h. Growth medium supplemented with a mixture of fluorescently tagged dextran and different concentrations of saponin was applied to the reservoir. After 10 min of incubation, the culture was washed three times in high glucose Dulbecco's modified eagle medium (DMEM) and imaged fluorescently. The above procedure was repeated on four duplicates. No fluorescence signal was observed in a saponin concentration of 2 μg/mL or lower (Figure 4a). When the concentration of saponin in the mixture was increased to 3 μg/mL (Figure 4b) we could identify a fluorescence signal confined to 70% $\pm$ 15% of the cells in direct contact with the NNA domain (nanoneedles open to the reservoir), indicating successful delivery of dextran through the nanoneedles into the cells. At a higher saponin level, 4 μg/mL, fluorescence appeared on 92% $\pm$ 7% of the cells in direct contact with the NNA, but also spread beyond the NNA to some cells growing on nearby blocked needles (Figure 4c). Remote cells growing on blocked needles (not shown) did not show any fluorescence, nor did cells growing on flat silicon.

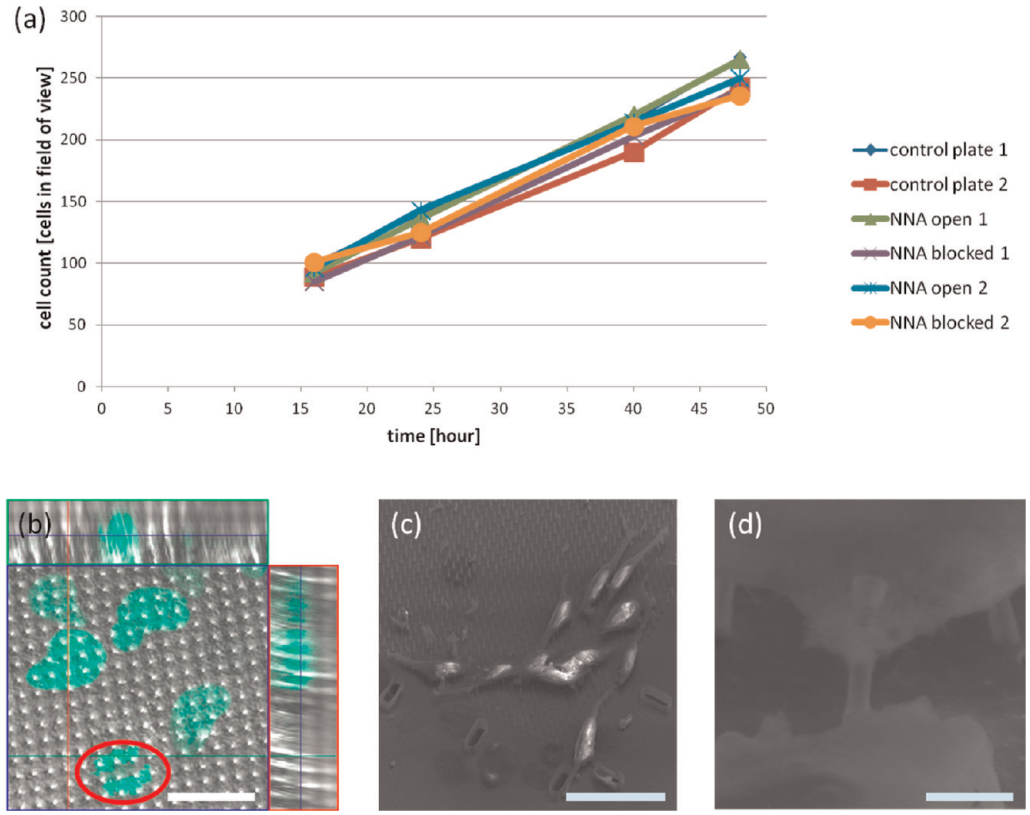

Figure 3. Cells growth on the nanoneedles. (a) HEK293 cell growth curves on normal tissue culture−plate (control) and on the NNA dies, 16−48 h after seeding at a density of 150,000 cells/mL. The number of cells in a 600 μm × 600 μm area as a function of time is shown for control cell culture dishes, NNA dies containing open and closed nanoneedles, and flat silicon domains. The cell population grows steadily. No difference in the growth rate is observed between cells grown on the dies and those that grew on standard cell culture plates. (b) Confocal image of HEK293 cells expressing nuclear eGFP. The figure depicts a *z*-section midlength along the needles. The cells span the entire length of the nanoneedles, with their nuclei engulfing some needles. The cell at the bottom of the figure, marked by a red circle, undergoes division. The side views show *z*-section reconstruction of the cells shown in the main figure. (c) SEM image of NIH3T3 cells fixated at the edge of the array. The cells localize themselves above the base of the needles. (d) Magnified SEM image of an NIH3T3 cell engulfing a nanoneedle. Scale bars: (b) 25, (c) 50, (d) 2 μm.

Saponin concentrations of 5 μg/mL and higher induced cell death during the hour that followed the reagent introduction. No fluorescence was observed in control cells cultured on standard cell culture plates, or in cells grown on flat perforated membranes. Finally, saponin levels below 5 μg/mL did not affect cell proliferation, vitality, and wellbeing on the NNA dies.

To determine the potential of the developed technique for repeated intracellular cargo administration we evaluated repeated delivery of dextran conjugated to different dyes to the same cells. As seen in Figure 5, after successfully passing Cascade Blue conjugated dextran we were also successful in transferring dextran conjugated with Texas Red dye to the same cells.

Cell Transfection. The NNA described above has proven an effective transfection tool. A plasmid encoding for Red Fluorescent Protein (RFP) has been delivered to cultured HEK293 cells. Two days after delivery, the cultured cells were imaged fluorescently on the NNA dies. As seen in Figure 6, most of the cells that grew on the NNA domain exhibited red fluorescence, indicating successful intracellular transfer of the plasmid and subsequent expression of the encoded RFP protein by the cells. Red fluorescence was also observed in some cells in the vicinity of the NNA domain. This finding may either indicate some plasmid delivery also to adjacent cells or, alternatively, migration of cells transfected in the NNA domain to adjacent areas. Importantly, cells in more distant domains of the die did not exhibit any detectable red fluorescence signal.

DISCUSSION

The fabrication technique described in this report is generic and robust. All etching steps rely on the selectivity of the various dry and wet etch processes with respect to silicon, silicon dioxide, and silicon nitride, leading to reproducible results at the nanoscale using conventional microfabrication technology. Mixing submicrometer high aspect ratio structures of different shapes on the same die is straightforward. The method is extendable, in principle, to any pair of materials to which selective etch processes exist. The new technique enables easy fabrication of the large number of hollow structures needed for a sizable cell

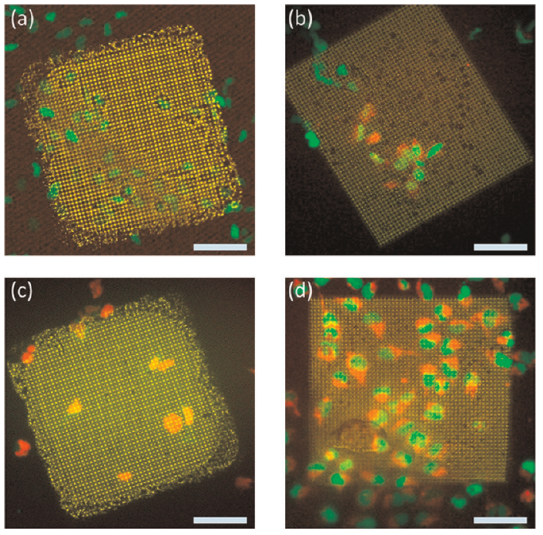

Figure 4. Dextran administration to cells. HEK293 cells expressing nuclear eGFP were grown on NNA dies. 3kD dextran conjugated with Texas Red dye mixed with different concentrations of saponin was applied to the reservoir at the back of the NNA domain (appearing yellow in the image). Ten minutes later, cells that grew on that domain exhibited cytoplasmatic red fluorescence, indicating successful dextran penetration to the cells: (a) 2 μg/mL saponin concentration, no internalization of dextran is observed; (b) 3 μg/mL saponin concentration, internalization of dextran is confined to cells in the NNA domain; (c) 4 μg/mL saponin concentration, internalization of dextran extends also to cells growing on blocked nanoneedles in the vicinity of the nanoneedles fed by the back reservoir, but not to distant cells; (d) 5 μg/mL saponin concentration, nonspecific administration of dextran is observed and cell vitality is compromised (see text). Scale bars: 70 μm.

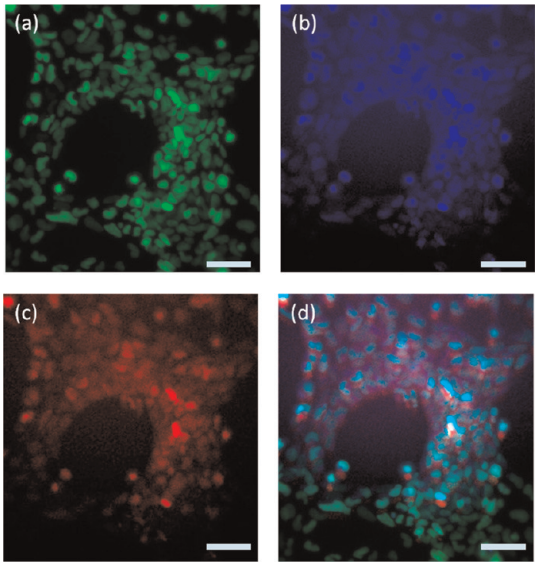

Figure 5. Repeated administration of dextran to HEK293 cells. (a) HEK293 cells expressing GFP in their nuclei. (b) The same cells after administration of dextran labeled with Cascade-Blue. (c) The same cells after subsequent administration of dextran labeled with Texas-Red. (d) Composite image of panels a–c. Cells at the lower part of the image grew on nanoneedles disconnected from the reservoir and hence fluoresced only in green. Cells in the rest of the image grew on needles open to the reservoir and hence fluoresced in all three colors. Scale bars: 50 μm.

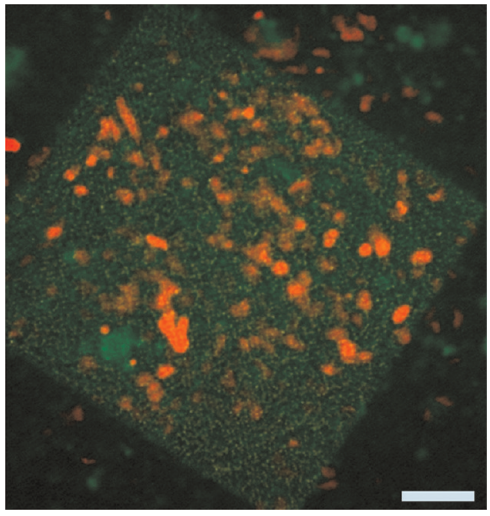

Figure 6. RFP expression in HEK293 cells, 48 h after successful delivery of the pIRES2 plasmid mixed with 3 μg/mL saponin. Expression of RFP is confined mostly to cells on the NNA fed by the back reservoir with some leakage to cells resting on nearby blocked needles (see text). Scale bar: 50 μm.

culture. Up-scaling to even larger areas is limited only by e-beam lithography of the etch mask. This gap can be mitigated by alternatives such as stamping and masking by colloids.

Selective administration of molecules to specific cells using the developed technique requires both saponin and nanoneedles. Saponin is known to promote pore formation in biological membranes. We hypothesize that the presence of saponin in the solution eases the penetration of target molecules into the cell by creating pores that are fine enough to maintain cell vitality. The concentration of saponin and target molecules decays rapidly with distance, reaching a negligible value outside the hollow NNA. The optimal saponin concentration, 3 μg/mL, is high enough to induce pores in nearby cells but too low to affect remote cells. Interestingly, a higher saponin concentration of 4 μg/mL enabled penetration of dextran and double-stranded DNA also into adjacent cells growing on blocked needles but not to cells growing on flat solid or perforated silicon. This result indicates that the interaction with needles enhances cell susceptibility to saponin and eventually, intracellular cargo delivery with no apparent effect on cell vitality and proliferation capacity. Since cargo delivery into cells was not observed on the flat perforated membranes of the device we hypothesize that the interaction with the nanoneedles has some mechanical effect on the cells, rendering them more susceptible to saponin.

CONCLUSION

A new high throughput method enabling the fabrication of hollow nanostructures was employed to produce large arrays of high-aspect-ratio nanoneedles

fed by a common reservoir. By combining the mechanical effects of these nanoneedles on the cells' membrane with localized concentrations of the reagent saponin we were able to demonstrate repeated administration of different biomolecules and efficient transfection to the same cells in a culture, with no effect on their long-term well being.

The developed method may bring a unique value to basic and translational cell biology by filling an important methodological gap. Specifically, the established delivery system facilitates repeated molecular interventions and allows targeting of specific intracellular processes in selected cells in a predetermined spatiotemporal manner. This ability may turn particularly useful for studies attempting to modify a subpopulation of cells within a larger population; *e.g.*, for studying cell-fate decisions and the role of cell-autonomous *versus* nonautonomous mechanisms in developmental biology. Similarly, the effects of altering the functional properties of specific cells (such as electrical properties) within a larger cellular network on the overall tissue activity may now be studied.

METHODS

The fabrication of nanoneedle arrays is detailed in the Supporting Information, S1.

Cleaning and Sterilization of NNA Dies. The NNA dies were cleaned and sterilized by dipping them in a freshly made hot (upon preparation, the mixture heats spontaneously to approximately 120 °C) "piranha" solution; a mixture of 2:1 H_2SO_4:H_2O_2. Piranha treatment ensured sterilization of the dies, rendered the surface hydrophilic, and eliminated needle clogging. After 10 min in piranha the samples were rinsed for 15 min in flowing doubly distilled water. Samples were used immediately after cleaning.

Passing Substances through the NNA. The NNA die was placed in a sample holder (see Supporting Information section S2 for detailed description) with its front side immersed in 50 μL of PBS. The holder was placed on the stage of an inverted microscope (Zeiss Axiovert 200) and 200 μL of solution containing either fluorescin or DNA in PBS was added to the reservoir. The passage of target molecules through the hollow nanoneedles to the solution in the front side of the die was evaluated several minutes after application (Figure 2).

Running DNA in Agarose Gel. Aliquots of 20 μL of DNA solution collected from the back reservoir, as well as samples collected near the front surface of the NNA, were run under 160 V in 1% agarose gel for 20 min. The resulting bands are depicted in Figure 2b.

Cell Culturing on NNA Dies. Dies were immersed in standard 12-well plates, and each well was filled with 1 mL of 4.5g/L DMEM supplemented with glutamine (2 mM), fetal calf serum (0.1 mL), penicillin (100 U), and G418 antibiotics (2 mg/mL). There were 250 000 cells added to each well. The plates were incubated at 37 °C, 5% CO_2 for 48 h.

Fixation for SEM Imaging. Specimens were washed twice in PBS, and then fixated with 2% glutaldehide solution for 30 min followed by three washes in cacodylate buffer at pH 7.4. To improve contrast, the cells were then labeled with osmium tetroxide, gradually transferred to ethanol, and critically point dried. Finally, the specimens were sputter-coated with chromium and imaged in a SEM (electron beam of a dual beam FEI Strata400S FIB machine). All reagents were purchased from Bar-Naor, Israel.

Administration of Fluorescently Tagged Dextran to Cells. HEK293 cells were cultured on the NNA dies to 80% confluence, reached after 48 h. A die was placed in the sample holder with its front side immersed in 50 μL DMEM solution. A 150 μL portion of DMEM supplemented with a mixture of 3kD Dextran-Texas Red conjugate (Sigma, Israel) and saponin (Sigma, Israel) were applied to the reservoir. The assembled sample holder was placed inside an incubator (37 °C, 7% CO_2) for 10 min. After 10 min the die was disassembled from the holder, washed three times to eliminate all remains of saponin and dye, reassembled, and imaged by an inverted ZEISS Axiovert 200 M microscope. For repeated administration, the same process was repeated with 3kD Dextran-Cascade Blue conjugate (Sigma, Israel).

Cell Transfection with DNA. pIsRes2-RFP-dsExpress plasmid (5.2 kbp) (Clontech), encoding for Red Fluorescent Protein (RFP), was added at a concentration of 5 ng/mL to the cell growth medium together with saponin (3 μg/mL). The solution was applied to the reservoir and the cells were allowed to incubate with it for 60 min. The sample holder was then disassembled and the die was transferred to cell growth plates, where the cells were left to grow for additional 48 h.

Conflict of Interest: The authors declare no competing financial interest.

Supporting Information Available: Details of the fabrication process, description of the sample holder for NNA dies, a theoretical estimate of the time scale needed for molecule diffusion through the nanoneedles, a time-lapse movie showing the fluorescence signal of fluorescin passing through the NNA die, confocal fluorescence images of cells growing on the NNA, and time-lapse movie of HEK293 cells expressing nucleic GFP cultured on an NNA die. This material is available free of charge *via* the Internet at http://pubs.acs.org.

Acknowledgment. This study was sponsored by the Russell Berrie Nanotechnology Institute at the Technion-Israel Institute of Technology, and the NNA dies were fabricated at the Technion's Micro-Nano Fabrication Unit (MNFU) facilities. The authors wish to thank Prof. Beni Geiger for his advice and the technical staff of MNFU for their support.

REFERENCES AND NOTES

1. Stephens, D. J.; Pepperkok, R. The Many Ways to Cross the Plasma Membrane. *Proc. Natl. Acad. Sci. U.S.A.* **2001**, *98*, 4295–4298.
2. Zhang, Y.; Yu, L.-C. Microinjection as a Tool of Mechanical Delivery. *Curr. Opin. Biotechnol.* **2008**, *19*, 506–510.
3. Zhang, Y.; Yu, L.-C. Single-Cell Microinjection Technology in Cell Biology. *BioEssays* **2008**, *30*, 606–610.
4. Cai, D.; Mataraza, J. M.; Qin, Z. H.; Huang, Z. P.; Huang, J. Y.; Chiles, T. C.; Carnahan, D.; Kempa, K.; Ren, Z. F. Highly Efficient Molecular Delivery into Mammalian Cells Using Carbon Nanotube Spearing. *Nat. Methods* **2005**, *2*, 449–454.
5. Kim, W.; Ng, J. K.; Kunitake, M. E.; Conklin, B. R.; Yang, P. Interfacing Silicon Nanowires with Mammalian Cells. *J. Am. Chem. Soc.* **2007**, *129*, 7228–7229.
6. Mann, D. G. J.; McKnight, T. E.; McPherson, J. T.; Hoyt, P. R.; Melechko, A. V.; Simpson, M. L.; Sayler, G. S. Inducible RNA Interference-Mediated Gene Silencing Using Nanostructured Gene Delivery Arrays. *ACS Nano* **2008**, *2*, 69–76.
7. McKnight, T. E.; Melechko, A. V.; Hensley, D. K.; Mann, D. G. J.; Griffin, G. D.; Simpson, M. L. Tracking Gene Expression after DNA Delivery Using Spatially Indexed Nanofiber Arrays. *Nano Lett.* **2004**, *4*, 1213–1219.
8. Pantarotto, D.; Singh, R.; McCarthy, D.; Erhardt, M.; Briand, J. P.; Prato, M.; Kostarelos, K.; Bianco, A. Functionalized Carbon Nanotubes for Plasmid DNA Gene Delivery. *Angew. Chem., Int. Ed.* **2004**, *43*, 5242–5246.
9. Park, S.; Kim, Y.-S.; Kim, W. B.; Jon, S. Carbon Nanosyringe Array as a Platform for Intracellular Delivery. *Nano Lett.* **2009**, *9*, 1325–1329.

10. Peckys, D. B.; Melechko, A. V.; Simpson, M. L.; McKnight, T. E. Immobilization and Release Strategies for DNA Delivery Using Carbon Nanofiber Arrays and Self-Assembled Monolayers. *Nanotechnology* **2009**, *20*, 145304–145312.
11. Rojas-Chapana, J.; Troszczynska, J.; Firkowska, I.; Morsczeck, C.; Giersig, M. Multiwalled Carbon Nanotubes for Plasmid Delivery into *Escherichia coli* Cells. *Lab Chip* **2005**, *5*, 536–539.
12. Shalek, A. K.; Robinson, J. T.; Karp, E. S.; Lee, J. S.; Ahn, D. R.; Yoon, M. H.; Sutton, A.; Jorgolli, M.; Gertner, R. S.; Gujral, T. S.; *et al.* Vertical Silicon Nanowires as a Universal Platform for Delivering Biomolecules into Living Cells. *Proc. Natl. Acad. Sci. U.S.A.* **2010**, *107*, 1870–1875.
13. Hallstrom, W.; Lexholm, M.; Suyatin, D. B.; Hammarin, G.; Hessman, D.; Samuelson, L.; Montelius, L.; Kanje, M.; Prinz, C. N. Fifteen-Piconewton Force Detection from Neural Growth Cones Using Nanowire Arrays. *Nano Lett.* **2010**, *10*, 782–787.
14. Jiang, K.; Fan, D.; Belabassi, Y.; Akkaraju, G.; Montchamp, J.-L.; Coffer, J. L. Medicinal Surface Modification of Silicon Nanowires: Impact on Calcification and Stromal Cell Proliferation. *ACS Appl. Mater. Interfaces* **2009**, *1*, 266–269.
15. Qi, S.; Yi, C.; Ji, S.; Fong, C.-C.; Yang, M. Cell Adhesion and Spreading Behavior on Vertically Aligned Silicon Nanowire Arrays. *ACS Appl. Mater. Interfaces* **2009**, *1*, 30–34.
16. Turner, A. M. P.; Dowell, N.; Turner, S. W. P.; Kam, L.; Isaacson, M.; Turner, J. N.; Craighead, H. G.; Shain, W. Attachment of Astroglial Cells to Microfabricated Pillar Arrays of Different Geometries. *J. Biomed. Mater. Res.* **2000**, *51*, 430–441.
17. Xie, C.; Hanson, L.; Xie, W. J.; Lin, Z. L.; Cui, B. X.; Cui, Y. Noninvasive Neuron Pinning with Nanopillar Arrays. *Nano Lett.* **2010**, *10*, 4020–4024.
18. Laforge, F. O.; Carpino, J.; Rotenberg, S. A.; Mirkin, M. V. Electrochemical Attosyringe. *Proc. Natl. Acad. Sci. U.S.A.* **2007**, *104*, 11895–11900.
19. Meister, A.; Gabi, M.; Behr, P.; Studer, P.; Voros, J. n.; Niedermann, P.; Bitterli, J.; Polesel-Maris, J. r. m.; Liley, M.; Heinzelmann, H.; *et al.* FluidFM: Combining Atomic Force Microscopy and Nanofluidics in a Universal Liquid Delivery System for Single Cell Applications and Beyond. *Nano Lett.* **2009**, *9*, 2501–2507.
20. Prinz, A. V.; Prinz, V. Y. Application of Semiconductor Micro- and Nanotubes in Biology. *Surf. Sci.* **2003**, *532−535*, 911–915.
21. Prinz, A. V.; Prinz, V. Y.; Seleznev, V. A. Semiconductor Micro- and Nanoneedles for Microinjections and Ink-Jet Printing. *Microelectron. Eng.* **2003**, *67−68*, 782–788.
22. Ahmad, M. R.; Nakajima, M.; Kojima, S.; Homma, M.; Fukuda, T. *In Situ* Single Cell Mechanics Characterization of Yeast Cells Using Nanoneedles Inside Environmental SEM. *IEEE Trans. Nanotechnol.* **2008**, *7*, 607–616.
23. McKnight, T. E.; Melechko, A. V.; Griffin, G. D.; Guillorn, M. A.; Merkulov, V. I.; Serna, F.; Hensley, D. K.; Doktycz, M. J.; Lowndes, D. H.; Simpson, M. L. Intracellular Integration of Synthetic Nanostructures with Viable Cells for Controlled Biochemical Manipulation. *Nanotechnology* **2003**, *14*, 551–556.
24. Yum, K.; Wang, N.; Yu, M. F. Nanoneedle: A Multifunctional Tool for Biological Studies in Living Cells. *Nanoscale* **2010**, *2*, 363–372.
25. Chen, X.; Kis, A.; Zettl, A.; Bertozzi, C. R. A. Cell Nanoinjector Based on Carbon Nanotubes. *Proc. Natl. Acad. Sci. U.S.A.* **2007**, *104*, 8218–8222.
26. Cuerrier, C. M.; Lebel, R.; Grandbois, M. Single Cell Transfection Using Plasmid Decorated AFM Probes. *Biochem. Biophys. Res. Commun.* **2007**, *355*, 632–636.
27. Han, S.; Nakamura, C.; Obataya, I.; Nakamura, N.; Miyake, J. Gene Expression Using an Ultrathin Needle Enabling Accurate Displacement and Low Invasiveness. *Biochem. Biophys. Res. Commun.* **2005**, *332*, 633–639.
28. Han, S. W.; Nakamura, C.; Obataya, I.; Nakamura, N.; Miyake, J. A Molecular Delivery System by Using AFM and Nanoneedle. *Biosens. Bioelectron.* **2005**, *20*, 2120–2125.
29. Obataya, I.; Nakamura, C.; Han, S.; Nakamura, N.; Miyake, J. Mechanical Sensing of the Penetration of Various Nanoneedles into a Living Cell Using Atomic Force Microscopy. *Biosens. Bioelectron.* **2005**, *20*, 1652–1655.
30. Vakarelski, I. U.; Brown, S. C.; Higashitani, K.; Moudgil, B. M. Penetration of Living Cell Membranes with Fortified Carbon Nanotube Tips. *Langmuir* **2007**, *23*, 10893–10896.
31. Adamo, A.; Jensen, K. F. Microfluidic Based Single Cell Microinjection. *Lab Chip* **2008**, *8*, 1258–1261.
32. Skold, N.; Hallstrom, W.; Persson, H.; Montelius, L.; Kanje, M.; Samuelson, L.; Prinz, C. N.; Tegenfeldt, J. O. Nanofluidics in Hollow Nanowires. *Nanotechnology* **2010**, *21*, 155301.
33. Persson, H.; Beech, J. P.; Samuelson, L.; Oredsson, S.; Prinz, C. N.; Tegenfeldt, J. O. Vertical Oxide Nanotubes Connected by Subsurface Microchannels. *Nano Res.* **2012**, *5*, 190–198.